01 Jun 2004

A Magnetic and Mössbauer Spectral Study of the Spin Reorientation in $NdFe_{11}Ti$ and $NdFe_{11}TH$

Cristina Piquer

Fernande Grandjean
Missouri University of Science and Technology, grandjeanf@mst.edu

Olivier Isnard

Viorel Pop

et. al. For a complete list of authors, see https://scholarsmine.mst.edu/chem_facwork/858

Recommended Citation

C. Piquer et al., "A Magnetic and Mössbauer Spectral Study of the Spin Reorientation in $NdFe_{11}Ti$ and $NdFe_{11}TH$," *Journal of Applied Physics*, vol. 95, no. 11 I, pp. 6308-6316, American Institute of Physics (AIP), Jun 2004.
The definitive version is available at https://doi.org/10.1063/1.1736333

A magnetic and Mössbauer spectral study of the spin reorientation in $NdFe_{11}Ti$ and $NdFe_{11}TiH$

Cristina Piquer[a] and Fernande Grandjean[b]
Department of Physics, B5, University of Liège, B-4000 Sart-Tilman, Belgium

Olivier Isnard[c]
Laboratoire de Cristallographie, CNRS, Associé à l'Université J. Fourier, BP 166X, F-38042 Grenoble Cedex, France and the Institut Universitaire de France, Maison des Universités, 103 Boulevard Saint-Michel, F-75005 Paris, Cedex, France

Viorel Pop
Laboratoire de Cristallographie, CNRS, Associé à l'Université J. Fourier, BP 166X, F-38042 Grenoble Cedex, France and the Department of Physics, Babes Bolyai University, R-400084 Cluj-Napoca, Romania

Gary J. Long[d]
Department of Chemistry, University of Missouri–Rolla, Rolla, Missouri 65409-0010

(Received 20 January 2004; accepted 10 March 2004)

The ac susceptibilities of $NdFe_{11}Ti$ and $NdFe_{11}TiH$, both of which crystallize with the $I4/mmm$ tetragonal $ThMn_{12}$-type structure, have been measured between 20 and 300 K and the results reveal spin reorientations at ~185 K and at 100 ± 1 K, respectively. The Mössbauer spectra of $NdFe_{11}Ti$ and $NdFe_{11}TiH$ have also been measured between 4.2 and 295 K and fits of the observed line shape profiles indicate that the spin-reorientations in both compounds correspond to a rotation from an axial orientation to a canted or basal orientation upon cooling. Both the low temperature canted or basal magnetic structures and the lowering of the spin-reorientation temperature upon hydrogenation result from the competing neodymium and iron magnetic anisotropies and differing relative second-, fourth-, and sixth-order contributions as a function of temperature and hydrogen content of the neodymium to the magnetic anisotropy energy. © *2004 American Institute of Physics.* [DOI: 10.1063/1.1736333]

I. INTRODUCTION

The $RFe_{11}Ti$ compounds, which crystallize in the tetragonal $ThMn_{12}$ structure with the $I4/mmm$ space group, have two main advantages as hard magnetic materials: (1) a high iron content which yields a high magnetization and (2) a relatively high Curie temperature.[1,2] In these compounds, the rare earth is located on the $2a$ crystallographic site, whereas the iron atoms are distributed over the $8i$, $8j$, and $8f$ sites. The $8i$ site is randomly occupied by the iron and titanium atoms whereas the $8j$ and $8f$ sites are fully occupied by iron.[2]

Neutron diffraction investigations[3,4] have indicated that, upon hydrogenation of the $RFe_{11}Ti$ compounds to form $RFe_{11}TiH$, the hydrogen is located on the $2b$ site, an octahedral site with two rare earth and four $8j$ iron near neighbors; the maximum hydrogen content per formula unit is one. The insertion of light interstitial atoms, such as hydrogen, carbon, or nitrogen, into the $RFe_{11}Ti$ structure has a beneficial effect on the magnetic properties of the compounds, increasing both their Curie temperatures and their saturation magnetizations.[5–7]

Hydrogen absorption can also yield important changes in the magnetic anisotropy of the $RFe_{11}Ti$ parent compounds and, specifically, hydrogenation can induce the appearance or disappearance of spin-reorientation transitions.[5,8–11] These spin reorientations have been studied extensively by magnetic and Mössbauer spectral measurements for the heavy rare-earth $RFe_{11}Ti$ compounds.[8–11] In this paper, the influence of hydrogenation on the spin reorientation in the presence of neodymium, a light rare-earth, is investigated[5,12–15] in detail in $NdFe_{11}Ti$.

$NdFe_{11}Ti$ is ferromagnetic with a Curie temperature between 550 and 600 K and exhibits[5,12–16] a spin reorientation at ~200 K. Above this temperature, the magnetic moments are aligned parallel to the c axis whereas, below this temperature, they cant away from the c axis. From ac susceptibility measurements, Kou *et al.* concluded[14] that this second-order spin reorientation takes place between a uniaxial and a conical magnetic phase.

A type-I first-order magnetization process was observed at 4.2 K and a critical field of 3.2 T when the applied field was applied along the c axis of $NdFe_{11}Ti$. Kou *et al.*[14] have developed a crystal field model in order to understand the spin reorientation and first-order magnetization processes. This model yielded a spin reorientation at 187 K and at a critical field of 2.7 T, results that are in good agreement with the experimental values. Further, the calculated canting angle, θ_c, increases with decreasing temperature from 0° at

[a]Permanent address: Instituto de Ciencia de Materiales de Aragon-CSIC, University of Zaragoza, E-50009 Zaragoza, Spain.
[b]Electronic mail: fgrandjean@ulg.ac.be
[c]Electronic mail: isnard@grenoble.cnrs.fr
[d]Electronic mail: glong@umr.edu

TABLE I. Lattice parameters, Curie temperatures, and saturation magnetizations.

Compound	a (Å)	c (Å)	c/a	V (Å^3)	T_C (K)	$M_s^{5\ \mathrm{K}}$ (μ_B)	$M_s^{300\ \mathrm{K}}$ (μ_B)
$NdFe_{11}Ti$	8.574(2)	4.794(1)	0.5591(2)	352.4(1)	551(4)	21.9(2)	20.1(2)
$NdFe_{11}TiH$	8.583(2)	4.815(1)	0.5610(2)	354.7(1)	614(4)	24.0(2)	21.6(2)

~200 K to 55° at 0 K. Similar conclusions have been reached[13] by Hu *et al.* who, by extrapolation from their crystal field model for $DyFe_{11}Ti$, predicted that the magnetic phase of $NdFe_{11}Ti$ is canted with a canting angle increasing from 0° at 200 K to a maximum of ~35° at 0 K. In contrast, Guslienko *et al.* have modeled[15] the magnetic properties of $NdFe_{11}Ti$ within the Asti and Bolzoni model[17] and concluded that the spin-reorientation transition observed at 189 K is a first-order transition with a discontinuous jump in the magnetization angle.

Another unusual feature of the magnetic properties of $NdFe_{11}Ti$ is the strong pressure dependence[18] of its Curie and spin-reorientation temperatures, temperatures that have slopes of −2.7 and −2.6 K/kbar, respectively.

The hydrogenation of $NdFe_{11}Ti$ to form $NdFe_{11}TiH$ expands[16] the unit-cell volume by 0.6% and increases the Curie temperature by 63 K, see Table I. This increase is substantially larger than the 22 K increase reported earlier;[19] the earlier smaller increase probably results from a hydrogen content of less than one hydrogen per mole.

There have been two investigations[20,21] of the iron-rich portion of the Nd–Fe–Ti phase diagram and three different phases have been identified, specifically, the $Nd(Fe,Ti)_{12}$, $Nd_2(Fe,Ti)_{17}$, and $Nd_3(Fe,Ti)_{29}$ solid solutions. All these phases have a crystal structure derived from the $CaCu_5$-type structure[22] but have different crystal symmetries. Namely, the first two solid solutions crystallize with the $ThMn_{12}$- and Th_2Zn_{17}-type structures, structures which exhibit tetragonal and rhombohedral unit cells, respectively. In contrast, the $Nd_3(Fe,Ti)_{29}$ solid solution exhibts[23,24] a much more complex structure with a monoclinic unit cell.

The aim of this paper is to report on a detailed study of the magnetic properties of highly pure $NdFe_{11}Ti$ and $NdFe_{11}TiH$ through ac magnetic susceptibility, thermomagnetic, magnetization, and iron-57 Mössbauer spectral studies and, more specifically, to determine the influence of hydrogenation on the spin-reorientation transition.

II. EXPERIMENT

Because all three of the Nd–Fe–Ti solid solutions mentioned earlier are structurally related, we have synthesized several Nd–Fe–Ti compounds with different iron to titanium stoichiometric ratios in order to ensure that only the pure $Nd(Fe,Ti)_{12}$ compound resulted. These compounds have been synthesized in a water-cooled copper crucible by melting 99.95% pure neodymium and titanium and 99.99% pure iron in a high frequency induction furnace. The resulting ingots were wrapped in a tantalum foil, annealed for five days at 1370 K in quartz tubes under an argon atmosphere, and quenched in water. On the basis of x-ray diffraction and thermomagnetic studies, a sample with an actual stoichiometry of $NdFe_{11.04}Ti_{0.96}$ was selected for further study. Only the tetragonal $ThMn_{12}$ phase was observed in the x-ray diffraction pattern and the sample was found to be single phase with only a small trace of α-iron. This sample will be referred to as $NdFe_{11}Ti$ throughout this paper.

The insertion of hydrogen into the $NdFe_{11}Ti$ crystal structure has been carried out through a solid–gas reaction described earlier and the hydrogen content was determined to be 1.0 ± 0.1 per formula unit by thermogravimetric methods.[16]

X-ray diffraction patterns were recorded with a Guinier–Hägg focusing camera with 1.9373 Å iron $K\alpha_1$ radiation; silicon powder was used as an internal standard. The lattice parameters and unit-cell volume are given in Table I.

The Curie temperatures were determined by magnetic measurements on a Faraday balance at a heating and cooling rate of 5°/min between 300 and 800 K. The samples were sealed in an evacuated silica tube both to avoid oxidation upon heating and to prevent hydrogen loss in the case of $NdFe_{11}TiH$. The magnetic properties were also measured between 4 and 300 K by using the extraction method in a field of up to 9 T. During all of these magnetic studies the microcrystalline powder was free to rotate in the applied field. The saturation magnetization, M_S, has been obtained by extrapolation of the isothermal magnetization to zero field. The resulting Curie temperatures and saturation magnetization values are given in Table I.

The low temperature ac magnetic susceptibilities have been obtained on a computer controlled mutual inductance susceptometer at an exciting field of 10^{-4} T and a frequency of 1 kHz. A lock-in amplifier was used to measure the complex susceptibility, $\chi_{ac}=\chi'-j\chi''$, where χ' is the initial susceptibility, a quantity which is related to the variation in the sample magnetization, and χ'' is nonzero if magnetic energy is absorbed by the sample. The temperature dependence of the real component, χ', and the imaginary component, χ'', of the ac susceptibility have been measured in order to determine the temperatures of the magnetic phase transitions. These measurements are very sensitive to the onset of the magnetic phase transition caused by changes in the anisotropy energy. The real portion of the ac susceptibility is determined predominantly by the changes in both the magnetic anisotropy energy and the domain wall energy.

The Mössbauer spectra have been measured between 4.2 and 295 K on a constant-acceleration spectrometer which utilized a rhodium matrix cobalt-57 source and was calibrated at room temperature with α-iron foil. The Mössbauer spectral absorbers contained 35 mg/cm^2 of powdered sample that had been sieved to a 0.045 mm or smaller diameter particle size. The low temperature spectra were measured in a Janis Super-Varitemp cryostat and the temperature was

controlled with a Lakeshore Cryogenics temperature controller with an accuracy of better than 1% of the observed temperature. The resulting spectra have been fit as discussed in the following and the estimated errors are at most ± 0.2 T for the hyperfine fields and their incremental changes, ± 0.01 mm/s for the isomer shifts and their incremental changes, and ± 0.02 mm/s for the quadrupole shifts and their incremental changes. The observed linewidths in the magnetic spectra were typically 0.38 ± 0.02 and 0.36 ± 0.02 mm/s for $NdFe_{11}Ti$ and $NdFe_{11}TiH$, respectively.

III. MAGNETIC RESULTS

Both $NdFe_{11}Ti$ and $NdFe_{11}TiH$ order ferromagnetically below Curie temperatures of 551 and 614 K, respectively. Although the increase in unit cell volume upon hydrogenation is smaller than in the analogous $RFe_{11}Ti$ compounds,[16] the approximately 10% increase in the Curie temperature is substantial. Further, the associated increase in the ordering temperature upon hydrogenation is a common feature of the $RFe_{11}Ti$ compounds.[16]

As may be seen in Table I, the saturation magnetization of $NdFe_{11}Ti$ is significantly increased upon hydrogenation both at 5 and 300 K. It is worth noting that, although an increase in the iron sublattice magnetization has been observed[3,16] in other $RFe_{11}Ti$ compounds, a reinforcement of the neodymium sublattice magnetization upon hydrogenation is also possible.

The ac susceptibility of $NdFe_{11}Ti$, see Fig. 1(a), exhibits a peak in χ' at a T_{SR} of ~185 K, a peak that corresponds to a spin reorientation. Similar results have been reported earlier[12,14] and attributed to a second-order spin reorientation arising from the competition between the neodymium and iron sublattice anisotropies. However, this reorientation was later reinterpreted[15] as corresponding to a first-order spin reorientation. Above T_{SR} and below the Curie temperature, the uniaxial magnetic anisotropy of the iron sublattice is dominant, whereas below T_{SR} the neodymium magnetocrystalline anisotropy becomes more important and promotes a reorientation of the magnetization. The shoulder in χ' that appears between 230 and 250 K is associated with domain-wall motion that is excited by the ac field. Similar behavior has been observed earlier[14] both in $NdFe_{11}Ti$ and in other rare-earth iron compounds,[25–27] such as $R_2Fe_{14}B$, $R_2Fe_{17}H_x$, and $CeFe_2$. At this point, it is uncertain why the χ'' exhibits only a small shoulder at 185 K and a major peak at 105 K but this behavior, which was also observed[14] earlier, may be associated, as will be discussed in the following, with the nature of the spin reorientation.

The ac susceptibility of $NdFe_{11}TiH$, see Fig. 1(b), exhibits a sharp peak in χ' at a T_{SR} of 100 ± 1 K, a peak that clearly corresponds to a spin reorientation. Further, a pronounced step beginning at ~200 K, a step that is similar to the shoulder observed in $NdFe_{11}Ti$, see Fig. 1(a), results from domain-wall motion. The spin reorientation observed in $NdFe_{11}TiH$ at 100 K is associated with an energy absorption which manifests itself as a sharp peak in the temperature dependence of χ'' at the inflexion point in the temperature dependence of χ', see Fig. 1(c).

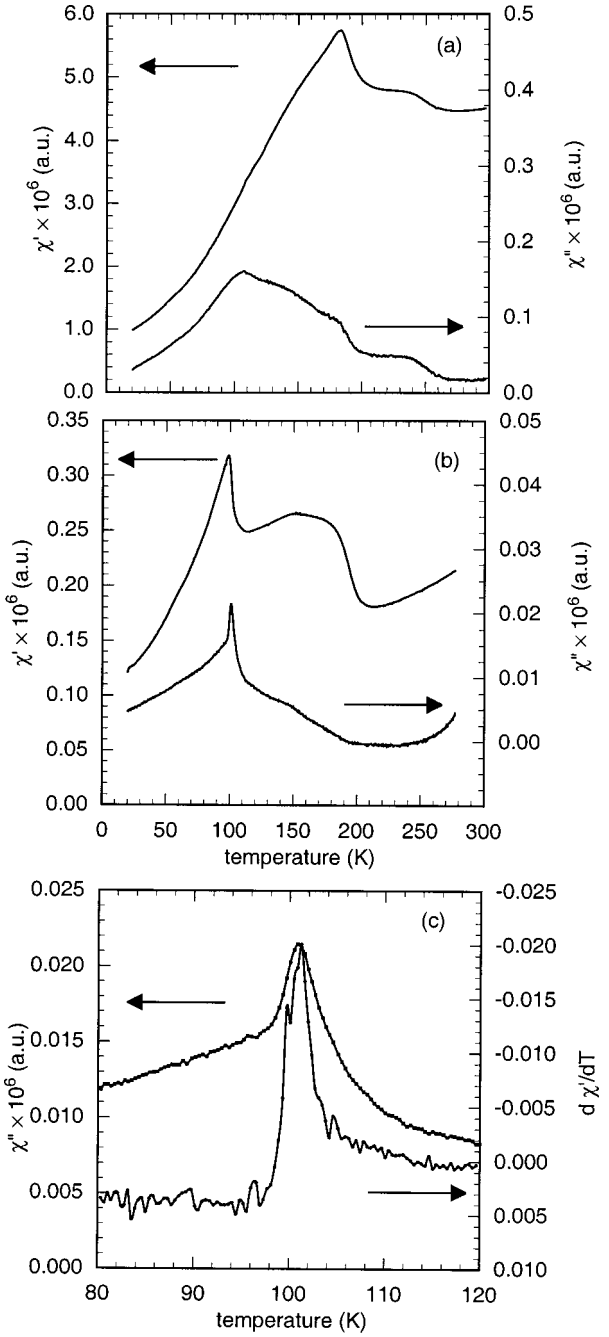

FIG. 1. The temperature dependence of the ac susceptibility of $NdFe_{11}Ti$ (a) and $NdFe_{11}TiH$ (b). The temperature dependence of χ'' and of the negative temperature derivative of χ' observed for $NdFe_{11}TiH$ (c).

Hence, in going from $NdFe_{11}Ti$ to $NdFe_{11}TiH$, the hydrogen insertion decreases the spin-reorientation temperature as a result of the influence of hydrogen upon the magnetocrystalline anisotropy. Indeed, previous investigations of the $RFe_{11}TiH$ compounds have shown[3,16] that the inserted hydrogen is a near neighbor of the rare earth and induces a significant change in the crystalline electric field gradient at the rare-earth site, a change that modifies the magnetic anisotropy. For example, an increase in the crystalline electric field gradient at the gadolinium site in $GdFe_{11}Ti$ has been observed[28] by Gd-155 Mössbauer spectroscopy.

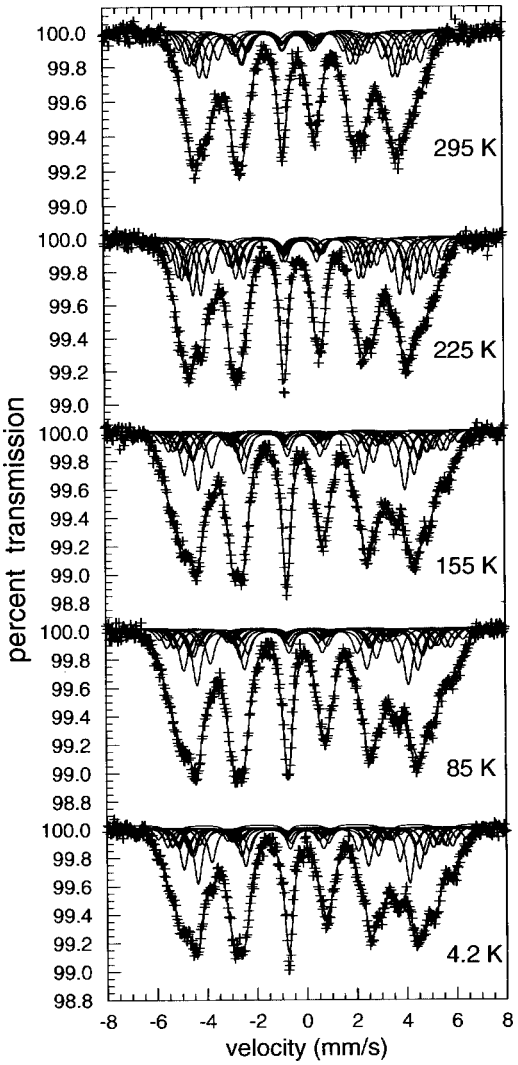

FIG. 2. The Mössbauer spectra of $NdFe_{11}Ti$ obtained between 4.2 and 295 K.

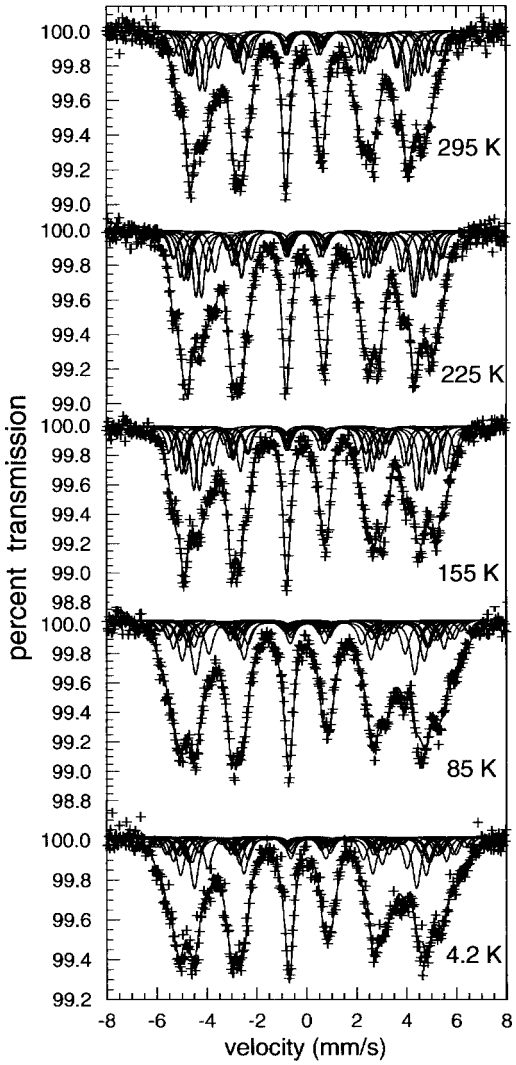

FIG. 3. The Mössbauer spectra of $NdFe_{11}TiH$ obtained between 4.2 and 295 K.

IV. MÖSSBAUER SPECTRAL MEASUREMENTS

The Mössbauer spectra of $NdFe_{11}Ti$ and $NdFe_{11}TiH$, obtained between 4.2 and 295 K, are shown in Figs. 2 and 3, respectively. A visual inspection of these figures indicates that the line shape profile of the spectra of $NdFe_{11}Ti$ changes between 155 and 225 K and that of $NdFe_{11}TiH$ between 85 and 155 K. These changes reflect the presence of a spin-reorientation transition within these temperature ranges, changes that are in good agreement with the spin-reorientation temperatures observed in Sec. III.

In $RFe_{11}Ti$ the iron and titanium atoms are randomly distributed over the $8i$ sites, whereas the $8j$ and $8f$ sites are fully occupied by iron atoms and, as a consequence, the iron atoms on the $8f$, $8i$, and $8j$ sites have a random distribution of near-neighbor environments, distributions that are assumed to be binomial in nature. Thus the $8i$ sextet is subdivided into three sextets with 6.47%, 10.79%, and 9.58% areas, and each of the $8f$ and $8j$ sextets are subdivided into three sextets with 11.51%, 15.34%, and 9.38% areas, sextets that represent spectral contributions from iron atoms with zero, one, and two or more titanium near neighbors, respectively.

Depending upon the magnetic structure, a further subdivision of these nine spectral components may be necessary. The point symmetry of the three iron sites in the $ThMn_{12}$ structure indicates that the principal axis of the electric field gradient, V_{zz}, is along the [100] direction for one half of the $8i$ and $8j$ sites, and along the [010] direction for the other half. For one half of the $8f$ sites, V_{zz} is along the [110] direction and for the other half V_{zz} is along the [1–10] direction. In the $RFe_{11}Ti$ compounds, the magnetization and, hence, the hyperfine field is along [001] in axial magnetic compounds, or along [100], [010], [110], or [1–10] in basal magnetic compounds. As a consequence, multiple relative orientations of the principal axis of the electric field gradient and of the hyperfine field result in different angles, θ, between these two directions and different quadrupole shifts and hyperfine fields can result.

If the $RFe_{11}Ti$ compound exhibits a uniaxial magnetic anisotropy, i.e., the easy magnetization direction is along the crystallographic c axis, then θ is 90° for the $8f$, $8i$, and $8j$ sites and no additional splitting of the nine spectral compo-

TABLE II. Mössbauer spectral hyperfine parameters[a] for $NdFe_{11}Ti$.

Parameter	T (K)	$8f$	$8i_1$	$8i_2$	$8j_1$	$8j_2$	Wt Av
$H_0(\Delta H)$, T	295	25.9(−2.8)	31.0(−1.8)	⋯	27.1(−2.4)	⋯	25.4
	225	27.5(−2.8)	33.7(−1.9)	⋯	29.0(−2.7)	⋯	27.2
	155	28.6(−2.9)	37.0(−2.4)	35.4(−2.0)	29.6(−1.7)	30.8(−2.5)	28.8
	85	29.1(−2.9)	37.7(−2.4)	35.8(−2.0)	30.0(−1.7)	31.4(−2.5)	29.4
	4.2	29.3(−2.9)	38.3(−2.8)	36.2(−2.0)	30.5(−1.8)	31.6(−2.5)	29.6
δ_0[b] $(\Delta\delta)$, mm/s	295	−0.161(0.005)	−0.002(−0.007)	⋯	−0.134(0.000)	⋯	−0.108
	225	−0.111(−0.002)	0.059(−0.006)	⋯	−0.077(−0.002)	⋯	−0.055
	155	−0.046(−0.024)	0.204(−0.076)	⋯	−0.007(−0.006)	⋯	0.003
	85	−0.028(−.022)	0.228(−0.071)	⋯	0.015(−0.006)	⋯	0.025
	4.2	−0.022(−0.024)	0.228(−0.070)	⋯	0.019(−0.009)	⋯	0.028
$\epsilon_0(\Delta\epsilon)$, mm/s	295	0.077(0.047)	0.132(−0.005)	⋯	−0.010(0.010)	⋯	0.078
	225	0.098(0.019)	0.112(0.010)	⋯	−0.042(0.001)	⋯	0.060
	155	−0.308(0.214)	0.015(−0.027)	0.004(−0.044)	0.245(−0.084)	0.025(0.134)	0.011
	85	−0.314(0.191)	0.032(−0.008)	0.012(−0.061)	0.313(−0.114)	−0.066(0.169)	0.001
	4.2	−0.335(0.207)	0.053(−0.053)	−0.039(−0.053)	0.337(−0.127)	−0.072(0.183)	0.002

[a]The numbers in parentheses are the incremental hyperfine parameters observed for one titanium near neighbor.
[b]Relative to room temperature α-iron foil.

nents described earlier is required. In contrast, if the compound exhibits basal or canted magnetic anisotropy and the magnetization lies in the [100] direction of the basal plane, or in the plane defined by the c axis and the [100] direction, there is a subdivision of the sextets representing the $8i$ and $8j$ sites but no subdivision for the $8f$ site. In such a case, each sextet assigned to the $8i$ and $8j$ sites has been subdivided into two sextets of equal relative areas, $8i_1$ and $8i_2$, and $8j_1$ and $8j_2$, with identical isomer shifts but different quadrupole shifts and, in some cases, slightly different hyperfine fields. When the easy magnetic direction is along [110] or in the plane defined by the [110] direction and the c axis, the situation is reversed and the $8f$ sextet is subdivided into two, $8f_1$ and $8f_2$, sextets of equal relative areas with identical isomer shifts but different quadrupole shifts and slightly different hyperfine fields; there is no further subdivision of the $8i$ and $8j$ sextets. This sextet subdivision is well established for the R_2Fe_{17} compounds, and it has been successfully applied in the analysis of the Mössbauer spectra of other $RFe_{11}TiH_x$ compounds.[8–11]

A given sextet is defined by three hyperfine parameters, the hyperfine field, H, the isomer shift, δ, and the quadrupole shift, ϵ. In order to build constraints into the model and to reduce the number of adjustable parameters, we have assumed that the three hyperfine parameters for each crystallographically inequivalent iron site change linearly with the number of titanium near neighbors, n, such that $H_n = H_0 + n\Delta H$, $\delta_n = \delta_0 + n\Delta\delta$, and $\epsilon_n = \epsilon_0 + n\Delta\epsilon$, where H_0, δ_0, and ϵ_0 are the hyperfine parameters with zero titanium near neighbors and ΔH, $\Delta\delta$, and $\Delta\epsilon$, are the changes in the hyperfine parameters for one additional titanium near neighbor. A similar linear dependence of the hyperfine field on the number of substitutional near-neighbor atoms has been successfully used[8–11,29–31] in the analysis of the Mössbauer spectra of both the $R_2Fe_{17-x}M_x$ solid solutions and $RFe_{11}TiH_x$ compounds.

Consequently, according to the above-presented model, for an axial magnetic phase the Mössbauer spectra have been fit with nine sextets, which have 18 hyperfine parameters, one line width, and one total absorption area. In contrast, for a nonaxial magnetic phase with the magnetization along [100] the Mössbauer spectra have been fit with 15 sextets, which have 26 hyperfine parameters, one line width, and one total absorption area. If the magnetization is along [110] the Mössbauer spectra have been fit with 12 sextets, which have 22 hyperfine parameters, one line width, and one total absorption area.

Herein, for both $NdFe_{11}Ti$ and $NdFe_{11}TiH$ below the spin-reorientation temperature, the further subdivision of the $8i$ and $8j$ sextets is essential for obtaining acceptable fits of the Mössbauer spectra as a function of temperature. As may be seen in Figs. 2 and 3, the fits are very good to excellent; the resulting hyperfine parameters are given in Tables II and III. Alternative fits with a subdivision of the $8f$ sextets were unsatisfactory. Consequently, we conclude that the Mössbauer spectra of $NdFe_{11}TiH$ observed below the spin-reorientation temperature are consistent either with the iron magnetic moments aligned along [100] within the basal plane of the tetragonal unit cell or contained within the plane defined by the [100] direction and the c axis of the unit cell.

In contrast to the present analysis, the earlier analyses of the Mössbauer spectra of $NdFe_{11}Ti$ were too simple. Indeed, the earlier Mössbauer spectra[12] of $NdFe_{11}Ti$ have been fit with two sextets for both the $8i$ and $8j$ sites, and one sextet for the $8f$ site at all temperatures, without any justification for the spectral deconvolution model. The hyperfine fields reported[12] at 80 and 295 K are smaller by 2 to 3 T than those given in Table II. The origin of this difference may be in the presence of some Nd_2Fe_{17} impurity in the earlier sample. The influence of the spin reorientation at 185 K on the Mössbauer spectra was not studied and the room temperature Mössbauer spectrum of $NdFe_{11}Ti$ was fit[7] with three sextets which were assigned to the three iron sites with no attempt to account for the titanium distribution or the orientation of the iron magnetic moments. The assignment of these three sextets to the three iron sites is compared with our assignments in Sec. V.

TABLE III. Mössbauer spectral hyperfine parameters[a] for $NdFe_{11}TiH$.

Parameter	T (K)	$8f$	$8i_1$	$8i_2$	$8j_1$	$8j_2$	Wt Av
$H_0(\Delta H)$, T	295	27.7(−2.7)	31.5(−1.5)	⋯	28.9(−2.9)	⋯	26.8
	225	29.1(−2.8)	33.5(−1.7)	⋯	30.6(−3.3)	⋯	28.2
	155	30.3(−3.2)	35.6(−2.1)	⋯	31.5(−3.1)	⋯	29.3
	85	30.6(−2.8)	38.5(−2.3)	35.5(−2.9)	33.9(−3.7)	31.1(−1.9)	30.2
	4.2	30.8(−2.9)	38.9(−2.5)	35.3(−2.9)	33.8(−3.7)	31.6(−1.9)	30.5
δ_0[b] $(\Delta\delta)$, mm/s	295	−0.110(0.016)	−0.032(0.020)	⋯	−0.070(−0.004)	⋯	−0.064
	225	−0.058(0.011)	0.024(0.017)	⋯	−0.020(−0.002)	⋯	−0.013
	155	−0.016(−0.002)	0.134(−0.010)	⋯	0.038(0.000)	⋯	0.041
	85	0.008(−0.013)	0.230(−0.054)	⋯	0.031(0.013)	⋯	0.060
	4.2	0.026(−0.013)	0.234(−0.054)	⋯	0.043(0.013)	⋯	0.072
$\epsilon_0(\Delta\epsilon)$, mm/s	295	0.001(0.161)	0.127(−0.034)	⋯	0.078(−0.066)	⋯	0.085
	225	0.038(0.148)	0.122(−0.034)	⋯	0.143(−0.128)	⋯	0.095
	155	0.034(0.149)	0.216(−0.051)	⋯	0.112(−0.059)	⋯	0.129
	85	−0.278(0.180)	−0.109(0.023)	0.117(−0.074)	0.409(−0.096)	−0.028(0.024)	−0.085
	4.2	−0.304(−0.188)	−0.022(0.002)	0.034(−0.040)	0.346(−0.080)	0.004(0.040)	−0.096

[a]The numbers in parentheses are the incremental hyperfine parameters observed for one titanium near neighbor.
[b]Relative to room temperature α-iron foil.

Because of the large number of parameters involved in the above-given fits, one would anticipate that it would be easy to obtain good spectral fits but that the resulting fits might be far from unique. Hence, in Sec. V we discuss the temperature dependencies of the hyperfine parameters and indicate how the temperature dependence helps to instill confidence in the spectral analysis, its physical applicability, and the extent to which it is unique. Extensive past experience of the authors indicates that it is not nearly as easy to obtain good fits of the observed spectra as might be anticipated especially when, as must be the case, physically acceptable changes in the hyperfine parameters with temperature are imposed upon the fits.

V. DISCUSSION

The assignment and temperature dependence of the three hyperfine fields with zero titanium near neighbors, and their weighted average, for $NdFe_{11}Ti$ and $NdFe_{11}TiH$ are shown in Figs. 4(a) and 4(b), respectively. A Wigner–Seitz cell analysis[32] of the three inequivalent iron sites in $RFe_{11}Ti$ and $RFe_{11}TiH$ indicates that the $8i$ site has 11.75 iron near neighbors, the largest average number of iron near neighbors, whereas the $8f$ and $8j$ iron sites both have nine iron near neighbors. Consequently, the sextets with the largest hyperfine field, H_0, have been assigned to the $8i$ site on the basis of both its relative contribution to the spectral absorption area and its iron near-neighbor environment. This assignment is further supported by the isomer shifts observed for the different sites, see the following. Because of both their identical constrained percentage spectral areas and their iron near-neighbor environments, it is not possible to unequivocally assign the $8f$ and $8j$ sextets on the basis of their fields and their assignment is based on their isomer shifts, see the following.

The solid lines in Fig. 4 are the result of a least-squares fit with[33]

$$H = H_0[1 - B_{3/2}(T/T_C)^{3/2} - C_{5/2}(T/T_C)^{5/2}],$$

where H_0 and T_C are the saturation field and magnetic ordering temperature, respectively. The $T^{3/2}$ term in this equation has its origin in the excitation of long-wavelength spin waves.[34] For $NdFe_{11}Ti$ $B_{3/2}$ and $C_{5/2}$ are between 0.02 and 0.06 and for $NdFe_{11}TiH$ they are between 0.4 and 0.9, respectively. It should be noted that the good fits obtained with

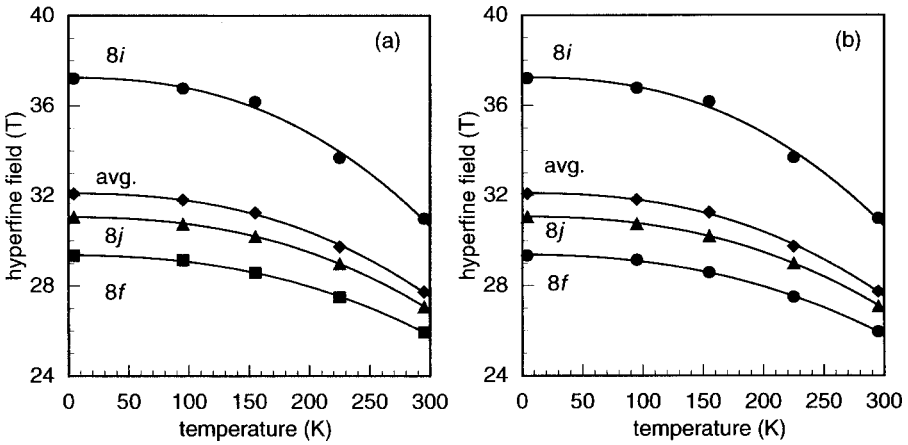

FIG. 4. The temperature dependence of the maximum hyperfine fields, H_0, at the three iron sites, and their weighted average, in $NdFe_{11}Ti$ (a) and in $NdFe_{11}TiH$ (b).

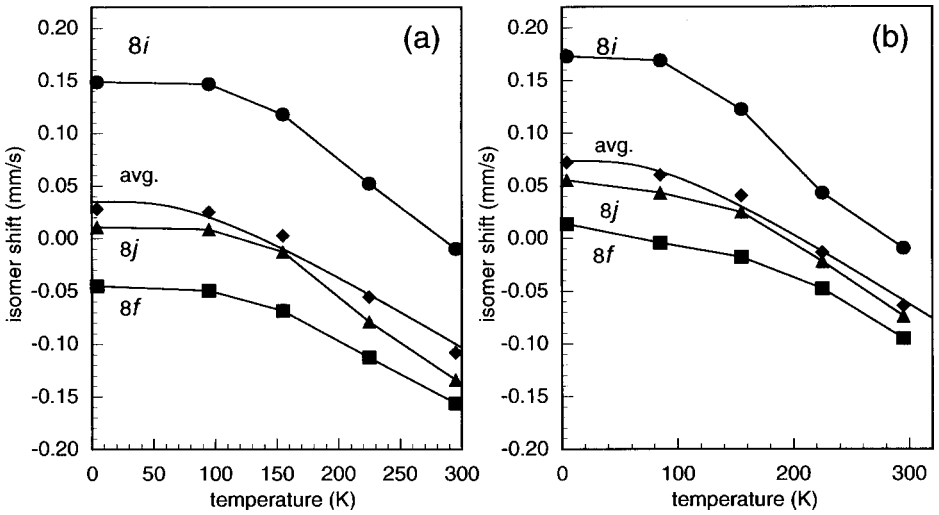

FIG. 5. The temperature dependence of the three site average isomer shifts, and their weighted average, in $NdFe_{11}Ti$ (a) and in $NdFe_{11}TiH$ (b).

the above-noted equation do not show any significant changes at the respective spin-reorientation temperatures of these compounds, see Fig. 4.

The changes in the hyperfine field per titanium near neighbor are between -2.9 ± 0.1 T and -2.5 ± 0.5 T for $NdFe_{11}Ti$ and -3.4 ± 0.4 T and -2.0 ± 0.5 T for $NdFe_{11}TiH$, where the errors reflect the variations in the changes with temperature between 4.2 and 295 K. The observed decreases in the hyperfine fields upon the replacement of one iron by one titanium near neighbor are similar to those observed[8–11,35] in the other $R Fe_{11}Ti$ compounds and their hydrides, and are within the range of -1.1 to -6 T observed[36,37] in a spinel oxide and in $Nd_2Fe_{16}Ti$, respectively.

The 4.2 K maximum hyperfine fields of the $8f$ and $8j$ iron sites in $NdFe_{11}Ti$ increase by ~ 2 T upon hydrogenation, whereas the $8i$ hyperfine field decreases by 0.3 T. At 295 K, the changes in hyperfine field upon hydrogenation are slightly different because of the concomitant increase in Curie temperature. The increase in the weighted average hyperfine field upon hydrogenation ranges between 0.5 and 1.5 T. Similar changes were observed in related $R Fe_{11}TiH_x$ compounds.[8–11,35]

Below the spin-reorientation temperatures, the difference between the maximum hyperfine fields assigned to the pair of magnetically inequivalent sites, $8i_1$ and $8i_2$, ranges between 1.6 and 2.1 T for $NdFe_{11}Ti$ and is ~ 3 T for $NdFe_{11}TiH$. The differences between the maximum hyperfine fields assigned to the $8j_1$ and $8j_2$ sites are slightly smaller at 1.2 ± 0.2 T for $NdFe_{11}Ti$ and 2.5 ± 0.3 T for $NdFe_{11}TiH$. The larger difference between the $8i$ hyperfine fields is also observed[8,10,11] in other $R Fe_{11}TiH_x$ compounds with basal magnetization. The only exception is $HoFe_{11}Ti$, whose $8i$ hyperfine field shows[9] a peculiar temperature behavior as a result of the increase in the $8i$ iron magnetic moment below the spin-reorientation temperature. The sextets associated with a pair of magnetically inequivalent sites have different hyperfine fields because of the differing orbital contributions to the field, as a consequence of the incomplete quenching[38,39] of the orbital moment, a quenching which results from the anisotropy in the spin–orbit coupling. Consequently, the stronger anisotropy observed in the $8i$ hyperfine field indicates that the orbital contribution to the $8i$ magnetic moment is larger than that of the $8j$ magnetic moment.

The assignment and the temperature dependence of the three site average isomer shifts, and their weighted average, are shown in Figs. 5(a) and 5(b), respectively. The site average isomer shifts have been calculated from the δ_n values weighted by the percent contribution given by the binomial distribution. In agreement with the Wigner–Seitz cell analysis[32] of the three inequivalent iron sites, the sequence of isomer shifts, $8i>8j>8f$, follows the sequence of Wigner–Seitz cell volumes. A similar correlation between the isomer shifts and the Wigner–Seitz cell volumes has been observed[8–11,30,31,35,40,41] in many $R Fe_{11}Ti$, $R_6Fe_{13}X$, and R_2Fe_{17} compounds. In contrast, the sequence of isomer shifts, $8j>8f>8i$, reported earlier[7] does *not* correspond to the sequence of Wigner–Seitz cell volumes.

The increase in the weighted average isomer shift upon hydrogenation is ~ 0.05 mm/s. A smaller increase in the $8i$ isomer shift than in the other two isomer shifts is observed[8–11,31] for all $R Fe_{11}TiH_x$ compounds, except when R is Tb. From the pressure dependence[18] of the Curie temperature, a ''negative'' pressure of -23 kbar was estimated[16] from the increase in Curie temperature upon hydrogenation of $NdFe_{11}Ti$. The increase in isomer shift upon hydrogenation may be compared with the pressure dependence of the isomer shift in α-iron[42] and in Gd_2Fe_{17}.[23] Changes in isomer shift of ~ 0.03 and ~ 0.04 mm/s are observed for a positive pressure of 25 kbar in α-iron and in Gd_2Fe_{17}, respectively. Hence, by extrapolation to a ''negative'' pressure these changes are very similar to the increase of ~ 0.05 mm/s observed herein.

The temperature dependence of the weighted average isomer shifts shown in Figs. 5(a) and 5(b) has been fit with the Debye model for the second-order Doppler shift.[43,44] For both compounds the resulting effective vibrating mass[43] is, as expected, 57 g/mol and the effective Mössbauer temperature is 350 ± 10 K. This temperature is typical of an intermetallic compound[45,46] and is very similar to that found for other $R Fe_{11}TiH_x$ compounds.[8–11,31,35]

The quadrupole shifts for the three inequivalent iron

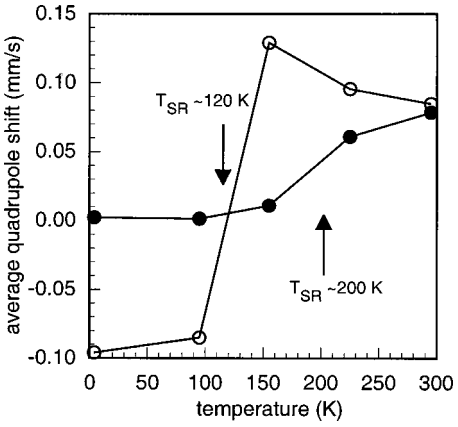

FIG. 6. The temperature dependence of the weighted average quadrupole shift in $NdFe_{11}Ti$, closed symbols, and in $NdFe_{11}TiH$, open symbols.

sites observed in the Mössbauer spectra of $NdFe_{11}Ti$ and $NdFe_{11}TiH$ are relatively small and range between -0.2 and 0.4 mm/s. Such small quadrupole shifts are expected because Mössbauer spectral studies[11,47] at 295 K of some related paramagnetic $R Fe_{11}Ti$ and $R Fe_{11}Mo$ compounds yield quadrupole splittings of, at most, 0.7 mm/s.

The temperature dependence of the average quadrupole shift in $NdFe_{11}Ti$ and $NdFe_{11}TiH$, see Tables II and III and Fig. 6, reflects the spin reorientations occurring in both compounds. Below the spin-reorientation temperatures, the average quadrupole shift is zero in $NdFe_{11}Ti$ and negative in $NdFe_{11}TiH$, and increases with increasing temperature up to a value of ~ 0.07 mm/s in the axial magnetic phase. Similar changes in the average value of the quadrupole splitting at the spin-reorientation temperature have also been observed in the Mössbauer spectra of the $R Fe_{11}TiH_x$ compounds, compounds which undergo spin-reorientation transitions.[9–11] More specifically, in the axial magnetic phase, the average quadrupole shift is positive at ~ 0.10 mm/s whereas in the planar magnetic phase, it is negative at ~ -0.05 mm/s.[9–11,31] Further, in a canted magnetic phase with a relatively large canting angle, as in $HoFe_{11}TiH$,[9] the average quadrupole shift is nearly zero. These results indicate that the average quadrupole shift directly reflects the magnetic anisotropy. By extrapolation of these observations to $NdFe_{11}Ti$ and $NdFe_{11}TiH$, the nearly zero value of the average quadrupole shift observed in $NdFe_{11}Ti$ below its spin-reorientation temperature indicates a canted magnetic phase with a canting angle close to 54.7°, a value that is in good agreement with the 60° value reported by Hu.[48] In a similar fashion, the average quadrupole shift of ~ -0.07 mm/s observed in $NdFe_{11}TiH$ below its spin-reorientation temperature indicates a canting angle of between 60° and 90° or even a planar magnetic phase.

In the $R Fe_{11}Ti$ compounds, and more generally in the $R Fe_{12-x}M_x$ solid solutions, the occurrence of a spin reorientation transition has also been found[14,15,48] to result from the importance of the fourth- and sixth-order anisotropy terms, terms which are the products of the rare-earth Stevens coefficient and of the crystal field parameters. There have been several attempts to determine the crystal field parameters in the $R Fe_{11}Ti$ compounds.[12,14,15,28,48–51] These parameters depend upon the nature of the rare earth, but for a given rare earth they will also vary because of the different approximations used by different authors. Even though the actual values must be accepted with care, they indicate that the inclusion of the fourth- and sixth-order crystal field parameters, together with the usually dominant second-order parameter, is necessary to explain the magnetic properties and more specifically the changes in the magnetic anisotropy of the $R Fe_{11}Ti$ compounds. For instance, the spin reorientation observed in $ErFe_{11}Ti$ results from the importance of the sixth-order term in the anisotropy energy.[52,53]

In the case of $NdFe_{11}Ti$, large values of the fourth- and sixth-order crystal-field parameters, A_4^m and A_6^0 have been reported.[14,15] In addition, neodymium is characterized by the second-, fourth-, and sixth-order Stevens coefficients, α_J, of -0.643×10^{-2}, β_J, of -2.911×10^{-4}, and γ_J, of -37.99×10^{-6}. Hence, the fourth- and sixth-order contributions to the magnetic anisotropy energy, which are the products of the crystal field parameters and the Stevens coefficients, cannot be neglected and are particularly important in determining the canted magnetic structure at low temperature. Hydrogen insertion is known[28] to increase the second order, A_2^0, crystal-field parameter but, to date, its influence upon the higher order crystal-field parameters is unknown. So, hydrogen insertion in $NdFe_{11}Ti$ to form $NdFe_{11}TiH$ is expected to reinforce the planar magnetic anisotropy of neodymium in agreement with the increase in canting angle deduced from the Mössbauer spectral results. Further, if hydrogen insertion changes the importance of the higher order terms relative to the second-order term in the magnetic anisotropy energy, the hydrogen insertion may also change the spin-reorientation temperature and the nature of the transition. Indeed, Hu has shown[48] that the energy surface in $NdFe_{11}Ti$, as a function of canting angle, exhibits two minima at 0 and 60° with an energy minima difference of 10 K separated by a barrier of ~ 20 K. At 4.2 K, the minimum at 60° is lower in energy and hence favored. In view of the small difference in minima energies and the small intervening energy barrier, it is not surprising that hydrogen insertion is capable of both changing the canting angle corresponding to the minima and the height of the energy barrier. On the basis of the Mössbauer spectral analysis, we believe that hydrogen insertion moves the lowest minimum at 4.2 K to a canting angle of $\sim 90°$ and, as is indicated by the lowering of T_{SR}, decreases the height of the energy barrier.

VI. CONCLUSIONS

The magnetic properties of $NdFe_{11}Ti$ and $NdFe_{11}TiH$ have been determined through combined ac magnetic susceptibility, thermomagnetic, and iron-57 Mössbauer spectral studies. A significant increase in both the Curie temperature and the saturation magnetization is obtained upon hydrogenation of $NdFe_{11}Ti$ to form $NdFe_{11}TiH$. The results indicate that $NdFe_{11}Ti$ and $NdFe_{11}TiH$ undergo a spin-reorientation transition at ~ 185 K and at 100 ± 1 K, respectively, from an axial magnetic phase at higher temperatures to a canted or basal magnetic phase at lower temperatures. The canted

magnetic structure of $NdFe_{11}Ti$ and $NdFe_{11}TiH$ and the lowering of the spin-reorientation temperature upon hydrogenation result from an interplay of the second-, fourth-, and sixth-order terms to the magnetic anisotropy energy.

The Mössbauer spectral study of $NdFe_{11}Ti$ supports the existence of a canted magnetic phase at low temperature and an axial phase at high temperature. The corresponding analyses of the spectra are consistent with the iron moments aligned parallel within the plane defined by the [100] direction and the *c* axis below the spin reorientation and with the iron moments parallel to the *c* axis above the spin reorientation. The Mössbauer spectral study of $NdFe_{11}TiH$ and the resulting hyperfine parameters indicate that it has a planar magnetic structure below its spin-reorientation temperature with the magnetic moments aligned along the [100] direction and an axial magnetic structure above its spin-reorientation temperature with the magnetic moments aligned along the [001] direction. Finally, the temperature dependence of the average quadrupole shift reveals itself as an excellent tool to detect the presence of a spin reorientation in the $RFe_{11}TiH_x$ compounds.

ACKNOWLEDGMENTS

The financial support of the University of Liège through Grant No. 2850006 is acknowledged with thanks. F.G. thanks the ''Fonds National de la Recherche Scientifique, Belgium,'' for Grant No. 9.456595. G.J.L. thanks the Francqui Foundation of Belgium for his appointment as a ''Chaire Francqui Interuniversitaire au titre étranger'' during the 2002-2003 academic year. This work was partially supported by the U.S. National Science Foundation through Grant No. INT-9815138, and the ''Centre National de la Recherche Scientifique, France'' through grant action initiative number 7418.

[1] H. Li and J. M. D. Coey, in *Handbook of Magnetic Materials* (North-Holland, Amsterdam, 1992), Vol. 6, p. 1, and references therein.
[2] K. H. J. Buschow, in *Electronic and Magnetic Properties of Metals and Ceramics, Part II*, Materials Science and Technology Series, Vol. 3B, edited by K. H. J. Buschow (VCH, Berlin, 1994), p. 451.
[3] O. Isnard, S. Miraglia, M. Guillot, and D. Fruchart, J. Alloys Compd. **275–277**, 637 (1998).
[4] A. Apostolov, R. Bezdushnyi, N. Stanev, R. Damianova, D. Fruchart, J. L. Soubeyroux, and O. Isnard, J. Alloys Compd. **265**, 1 (1998).
[5] S. A. Nikitin, I. S. Tereshina, V. N. Verbetsky, and A. A. Salamova, J. Alloys Compd. **316**, 46 (2001).
[6] J. L. Soubeyroux, D. Fruchart, O. Isnard, S. Miraglia, and E. Tomey, J. Alloys Compd. **219**, 16 (1995).
[7] Z. W. Li, X. Z. Zhou, and A. H. Morrish, J. Phys.: Condens. Matter **4**, 10409 (1992).
[8] C. Piquer, R. P. Hermann, F. Grandjean, G. J. Long, and O. Isnard, J. Appl. Phys. **93**, 3414 (2003).
[9] C. Piquer, F. Grandjean, G. J. Long, and O. Isnard, J. Alloys Compd. **353**, 33 (2002).
[10] C. Piquer, O. Isnard, F. Grandjean, and G. J. Long, J. Magn. Magn. Mater. **265**, 156 (2003).
[11] C. Piquer, R. Hermann, F. Grandjean, O. Isnard, and G. J. Long, J. Phys.: Condens. Matter **15**, 7395 (2003).
[12] B. P. Hu, H. S. Li, J. P. Gavigan, and J. M. D. Coey, J. Phys.: Condens. Matter **1**, 755 (1989).
[13] B. P. Hu, H. S. Li, J. M. D. Coey, and J. P. Gavigan, Phys. Rev. B **41**, 2221 (1990).
[14] X. C. Kou, T. S. Zhao, R. Grössinger, H. R. Kirchmayr, X. Li, and F. R. de Boer, Phys. Rev. B **47**, 3231 (1993).
[15] K. Yu. Guslienko, X. C. Kou, and R. Grössinger, J. Magn. Magn. Mater. **150**, 383 (1995).
[16] O. Isnard, J. Alloys Compd. **356–357**, 17 (2003).
[17] G. Asti and F. Bolzoni, J. Magn. Magn. Mater. **20**, 29 (1980).
[18] Z. Arnold, M. R. Ibarra, L. Morellon, P. A. Algarabel, and J. Kamarad, J. Magn. Magn. Mater. **157–158**, 81 (1996).
[19] Ph. Oleinek, D. Eckert, K. H. Müller, and L. Schultz, J. Phys. D **32**, 1578 (1999).
[20] A. Margarian, J. B. Dunlop, R. K. Day, and W. Kalceff, J. Appl. Phys. **76**, 6153 (1994).
[21] T. S. Jang and H. H. Stadelmaier, J. Appl. Phys. **67**, 4957 (1990).
[22] B. P. Hu, H. S. Li, and J. M. D. Coey, J. Appl. Phys. **67**, 4838 (1990).
[23] F. S. Li, J. J. Sun, C. L. Yang, R. J. Zhou, B. G. Shen, H. Micklitz, and M. M. Abd-Elmeguid, Hyperfine Interact. **94**, 1959 (1994).
[24] Z. Hu and W. B. Yelon, Solid State Commun. **91**, 223 (1994).
[25] E. H. Büchler, M. Hirsher, and H. Kronmüller, in *Interstitial Intermetallic Alloys*, edited by G. J. Long, F. Grandjean, and K. H. J. Buschow (Kluwer, Dordrecht, 1994), p. 521.
[26] L. M. Garcia, J. Bartolomé, F. J. Lazaro, C. De Francisco, J. M. Munoz, and D. Fruchart, J. Magn. Magn. Mater. **140–144**, 1049 (1995).
[27] F. Grandjean, O. Isnard, D. Hautot, and G. J. Long, Phys. Rev. B **63**, 014406 (2000).
[28] O. Isnard, P. Vulliet, J. P. Sanchez, and D. Fruchart, J. Magn. Magn. Mater. **189**, 47 (1998).
[29] G. J. Long, G. K. Marasinghe, S. Mishra, O. A. Pringle, Z. Hu, W. B. Yelon, D. P. Middleton, K. H. J. Buschow, and F. Grandjean, J. Appl. Phys. **76**, 6731 (1994).
[30] D. Hautot, G. J. Long, P. C. Ezekwenna, F. Grandjean, D. P. Middleton, and K. H. J. Buschow, J. Appl. Phys. **83**, 6736 (1998).
[31] C. Piquer, O. Isnard, F. Grandjean, and G. J. Long, J. Magn. Magn. Mater. **263**, 235 (2003).
[32] L. Gelato, J. Appl. Crystallogr. **14**, 141 (1981).
[33] H. N. Ok, K. S. Baek, and C. S. Kim, Phys. Rev. B **24**, 6600 (1981).
[34] C. Herring and C. Kittel, Phys. Rev. **81**, 869 (1951).
[35] G. J. Long, D. Hautot, F. Grandjean, O. Isnard, and S. Miraglia, J. Magn. Magn. Mater. **202**, 100 (1999).
[36] J. L. Dormann, Rev. Phys. Appl. **15**, 1113 (1980).
[37] F. Grandjean, P. C. Ezekwenna, G. J. Long, O. A. Pringle, Ph. L'Héritier, M. Ellouze, H. P. Luo, and W. B. Yelon, J. Appl. Phys. **84**, 1893 (1998).
[38] M. T. Averbuch-Pouchot, R. Chevalier, J. Deportes, B. Kebe, and R. Lemaire, J. Magn. Magn. Mater. **68**, 190 (1987).
[39] M. Kawakami, T. Hihara, Y. Koi, and T. Wakiyama, J. Phys. Soc. Jpn. **33**, 1591 (1972).
[40] D. Hautot, G. J. Long, F. Grandjean, O. Isnard, and S. Miraglia, J. Appl. Phys. **86**, 2200 (1999).
[41] O. Isnard, G. J. Long, D. Hautot, K. H. J. Buschow, and F. Grandjean, J. Phys.: Condens. Matter **14**, 12391 (2002).
[42] D. L. Williamson, S. Bukshpan, and R. Ingalls, Phys. Rev. B **6**, 4194 (1972).
[43] R. H. Herber, in *Chemical Mössbauer Spectroscopy*, edited by R. H. Herber (Plenum, New York, 1984), p. 199.
[44] G. J. Long, D. Hautot, F. Grandjean, D. T. Morelli, and G. P. Meisner, Phys. Rev. B **60**, 7410 (1999); **62**, 6829 (2000).
[45] F. Grandjean, O. Isnard, and G. J. Long, Phys. Rev. B **65**, 064429 (2002).
[46] G. J. Long, O. Isnard, and F. Grandjean, J. Appl. Phys. **91**, 1423 (2002).
[47] F. Grandjean, R. P. Hermann, and G. J. Long (unpublished).
[48] B. P. Hu, Ph.D. thesis, University of Dublin, 1990.
[49] C. Abadia, P. A. Algarabel, B. Garcia-Landa, M. R. Ibarra, A. del Moral, N. V. Kudrevatykh, and P. E. Markin, J. Phys.: Condens. Matter **10**, 349 (1998).
[50] M. D. Kuzmin, J. Appl. Phys. **88**, 7217 (2000).
[51] O. Isnard, M. Guillot, S. Miraglia, and D. Fruchart, J. Appl. Phys. **79**, 5542 (1996).
[52] A. V. Andreev, V. Sechovsky, N. V. Kudrevatykh, S. S. Sigaev, and E. N. Tarasov, J. Less-Common Met. **144**, L21 (1988).
[53] I. S. Tereshina, S. A. Nikitin, V. N. Nikiforov, L. A. Ponomarenko, V. N. Verbetsky, A. A. Salamova, and K. P. Skokov, J. Alloys Compd. **345**, 16 (2002).